Current-Driven Resonances in Magnetic Multilayers

M. Tsoi,[1,2,3] V. Tsoi,[2] J. Bass,[3] A. G. M. Jansen,[1] and P. Wyder[1]

[1]*Grenoble High Magnetic Field Laboratory, Max-Planck-Institut für Festkörperforschung and Centre National de la Recherche Scientifique, BP 166, F-38042 Grenoble Cedex 9, France*

[2]*Institute of Solid State Physics RAS, 142432 Chernogolovka, Moscow Region, Russia*

[3]*Department of Physics and Astronomy, Michigan State University, East Lansing, Michigan 48824-1116*

(Received 28 July 2002; published 21 November 2002)

We describe complex variations in resistance of a Co/Cu multilayer, generated by injection of an adjustable dc current density ($\sim 10^9$ A/cm^2) via a point contact. We attribute these variations to coupling of current-induced spin waves to lattice vibrations, leading especially to current-driven resonant excitations of phonons. We propose a simple model to explain the observed structured behavior of the variations as a function of the applied current and magnetic field.

DOI: 10.1103/PhysRevLett.89.246803 PACS numbers: 73.40.Jn, 72.25.Ba, 72.55.+s, 76.50.+g

In accordance with the original predictions [1–3], injection of a large electrical current density into a magnetic multilayer has been shown to produce steps in electrical resistance (or peaks in derivative resistance) corresponding to generation of magnons or reversal of layer magnetizations [4–7]. These initial observations of current-induced magnons and magnetization switching have stimulated a large amount of theoretical [8–25] and experimental [26–37] work on a subject that combines interesting fundamental science with the promise of application to high-speed, high-density magnetic recording and storage.

Two of these studies [4,7] reported additional "structure" in resistance of magnetic multilayers that has not yet been explained [8–25]. In this paper we present a much more complete study of such additional structure as a function of both applied magnetic field B and injected current density j. Based upon both theoretical predictions [2,8] and experimental evidence [31] that current creates at least partially coherent magnons, we argue that the additional structure is due to resonant phonon, spin-wave, and magnetoacoustic modes, i.e., that the coupling of current-driven spin waves to sound waves allows the excitation of phonons by an electric current. We also propose a model to explain how and why particular modes are excited.

Our samples were sputtered $(\mathrm{Co/Cu})_N$ multilayers with bilayer number N ranging from 20–50 and layer thicknesses $t_{\mathrm{Co}} = 1.5$ nm and $t_{\mathrm{Cu}} = 2.0$–2.2 nm (for details see Refs. [4,30]). We induce spin waves, or "magnons," by means of a high current density ($\sim 10^9$ A/cm^2) injected into the multilayer film through a point contact between a sharpened Ag tip and the film. Such an unbounded geometry—point contact to a continuous multilayer film—is equivalent to a bounded geometry where the multilayer is replaced by a pillar structure (alternating ferromagnetic and nonmagnetic disks) [9,27,28,32]. Small portions of magnetic layers under the point contact, where the current density is high, play the role of ferromagnetic disks in the pillar. At helium temperature (4.2 K), we have measured the current-voltage (I-V) characteristics, and their derivatives, of point contacts at different magnetic fields B applied perpendicular to the layers.

We and others have observed a step increase in resistance of such contacts at a certain value of the bias current $I^*(B)$ corresponding to the onset of current-driven magnon generation. I^* was found to increase linearly with B, thereby dividing the I-B plane into two regions, where the multilayer is excited (at high currents $I > I^*$) or unexcited (at low currents $I < I^*$). Frequencies of magnons excited above this current threshold could be probed by external high-frequency radiation [31]. On some occasions, however, more elaborate structures in contact resistance have been reported as a function of either magnetic field B for fixed dc bias current I or I for fixed B [4,7]. These complex structures observed in some point contacts are the focus of the present work. To elucidate the source of these structures, we have examined how they vary with both B and I. An example of such behavior is illustrated in Fig. 1, where the solid lines show the variation of the derivative contact resistance dV/dI as a function of I for a series of values of B. Peaks in dV/dI correspond to step increases in the static contact resistance $R = V/I$. Some $dV/dI(I)$ traces have more than one peak evolving with magnetic field in a regular fashion. At higher bias some of the traces also have dips in dV/dI, which correspond to step decreases in R. Behaviors compatible with those shown have also been observed with other contacts.

Filled (open) symbols in Fig. 2 show the values of $I(B)$ where we observe peaks (dips) in the $dV/dI(I)$ spectra (the sizes of symbols are indicative of the peak/dip amplitude). Note that all the singularities in contact resistance occur above the current threshold $I^*(B)$ (AA' line in Fig. 2), i.e., when the current is exciting magnons in the multilayer. The locations of these singularities in I vary linearly with B (indicated by solid lines and dashed lines in Fig. 2). However, there are deviations from these linear

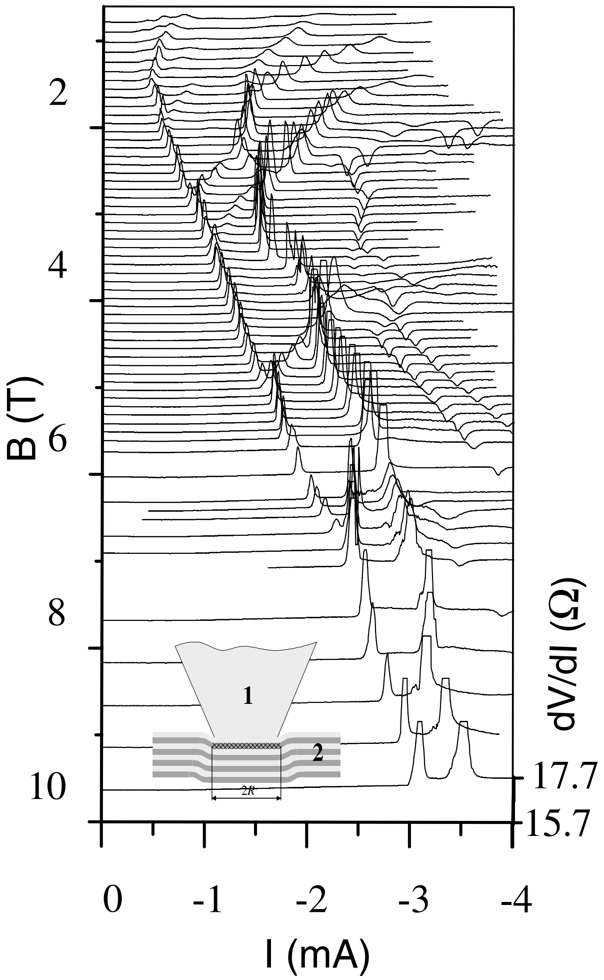

FIG. 1. Variation of the derivative contact resistance dV/dI as a function of dc bias current I for a series of magnetic fields. Solid lines show the point contact $dV/dI(I)$ spectra for a series of magnetic fields in the range 1–10 T. Peaks in dV/dI correspond to step increases in the static contact resistance $R = V/I$. Some of the $dV/dI(I)$ traces have more than one peak evolving with magnetic field in a regular fashion. At higher bias some of the traces also have dips in dV/dI, which correspond to step decreases in R. The inset shows the scheme of the resonator. In the process of making contact, the Ag tip (1) squeezes into the magnetic multilayer (2). The small portion of a Co layer (shaded) right under the contact may be viewed as a circular membrane of radius R (resonator).

dependences near intersections between lines with positive and negative slopes. These deviations are also accompanied by increases in the peak amplitudes. The peaks of maximum amplitude are indicated by line MM', which has a positive slope and is almost parallel to the threshold $I^*(B)$. In contrast, small peaks are located on the lines that have negative slopes and originate at this threshold. Finally, lines indicating the locations of dips (dashed lines in Fig. 2) have both positive and negative slopes similar to those indicating peak locations.

We attribute the observed variations in the contact resistance to the resonance excitation of spin waves and

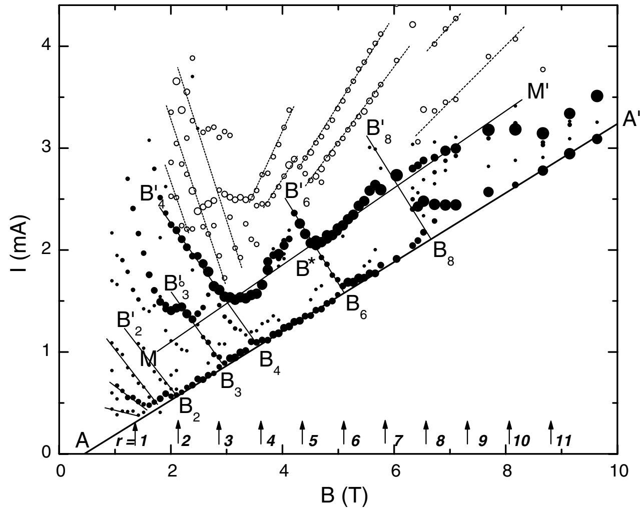

FIG. 2. Phase diagram for current-induced excitations. Filled (open) symbols show the values of $I(B)$ where we observe peaks (dips) in the $dV/dI(I)$ spectra. The sizes of the symbols are indicative of the peak/dip amplitude. Note that all the singularities in contact resistance occur above the current threshold $I^*(B)$ (AA' line), i.e., when the current is exciting magnons in the multilayer. The arrows indicate the values of magnetic field B^r corresponding to the excitation of magnons with $\omega_m = \omega^r_{\text{ph}}$ at the threshold $I^*(B)$ for $r = 1, 2, \ldots, 11$.

phonons by an electric current. First, we note that local heating of the sample associated with high bias currents results in a complex current- and temperature-induced excitation of noncoherent magnons and phonons. In contrast, we attribute the present singularities in point-contact characteristics to current-driven excitation of coherent phonon and magnon modes. We are concerned with the phenomena expected to occur when spin waves (magnons) are coupled to lattice vibrations (phonons). Existing theoretical analyses of the magnon generation by an electric current [1–25] do not take account of magnon-phonon coupling. Real systems, however, have such coupling, which leads to a displacement of the ions accompanying the spin oscillations and vice versa [38]. In addition to exciting magnons, a large current should, thus, also excite phonons. The additional dissipation of energy associated with such a current-driven generation of phonons should give an increase in resistance. In practice, the coupling between spin and elastic waves is weak and is important only under certain resonance conditions, where the changes in resistance are most pronounced [39].

In our experiments, the current excites a small portion of a Co layer right under the contact (hereafter referred to as an excited ferromagnet) [9,31]. At the contact, the Ag tip squeezes into the multilayer, thereby favoring a configuration shown in the inset of Fig. 1. Here the excited ferromagnet may be viewed as a membrane, or resonator (shaded in Fig. 1). We do not yet have a rigorous expression for the frequencies of the normal modes of vibration of such a membrane surrounded by other layers. In the simplest case of a circular membrane in vacuum, where the deflected surface of the membrane is symmetric with respect to the center of the circle and fixed at the boundary, the frequencies of the natural modes of vibration are given by [40]

$$\omega_{\rm ph}^{r} = \frac{\alpha_r}{R}\sqrt{\frac{S}{\rho h}}, \tag{1}$$

where R is the membrane radius, S the uniform tension per unit length of its boundary, h the membrane thickness, and ρh the mass per unit area; the mode number r denotes the number of nodal circles, at which deflections of the membrane are zero during vibration. The constants α_r ($r = 1, 2, \dots$) can be found numerically [40].

Generation of phonons by an electric current is most effective when the frequency of the current-driven magnons ω_m equals the frequency of one of the phonon modes $\omega_{\rm ph}^{r}$. Since the magnon frequency ω_m can be tuned by varying the applied magnetic field B and/or current I [1,2,31], excitation of a given phonon mode occurs at a certain value of the applied magnetic field. In Fig. 2, the arrows indicate the values of magnetic field B^r corresponding to the excitation of magnons with $\omega_m = \omega_{\rm ph}^{r}$ at the current threshold $I^*(B)$ for $r = 1, 2, \dots, 11$. The resonant dissipation of energy associated with generation of a given phonon mode should result in an increase in resistance. At higher bias currents, the increase in resistance is expected to occur at lower applied fields, thus following the contours of constant frequency, which have negative slopes in the I-B plane [31].

Our data are consistent with the above analysis (see Figs. 1 and 2). Additional peak structures in $dV/dI(I)$ start to develop around the threshold current I^* at characteristic values B^r of the applied magnetic field and then shift to higher values of the bias current I when the field is reduced below B^r. This peak structure corresponds to an upward step in the static contact resistance $R = V/I$. Filled circles in Fig. 2 show that the value of I where the step occurs shifts linearly with B. In this interpretation, lines B_iB_i' in Fig. 2 correspond to the excitation of phonon modes $\omega_{\rm ph}^{r}$ with $r = i$. The resonance field B^r of the $r = 1$ mode is smaller than the saturation field $B_S \sim 1.5$ T of the multilayer. This case is out of the scope of the present paper and will be published elsewhere [41]. Modes $r = 5$ and $r = 7$ may be suppressed by defects in the multilayer. Finally, distortions of the membrane (< 1 nm from circular shape) might be responsible for suppression of modes 11 and higher.

In addition to acoustic (phonon) resonances that we observe when $\omega_m = \omega_{\rm ph}^{r}$, one might also expect to see the resonance of spin waves (magnons) when the magnon wavelength λ_m is comparable to the size of the resonator R. We have previously shown [31] that the wave number ($k_m = 2\pi/\lambda_m$) of the current-induced magnons increases with increasing bias current I. By varying I and B, we thus can tune both ω_m and k_m. For instance, moving along the line B_6B_6' in Fig. 2, we keep exciting magnons at the same frequency; however, the magnon wave number k_m increases with I. At B^*, the acoustic resonance line B_6B_6' crosses the magnon resonance line MM'. The potential energy of the current-driven magnons excited at B^* is reduced by 25 GHz (~ 0.1 meV) if compared to those excited at the current threshold (B_6 in Fig. 2). Assuming that at B_6 we excite spin waves with small wave numbers k_m, e.g., corresponding to wavelengths $\lambda_m = 2\pi/k_m$ of the order of contact size $2R \approx 12$ nm [9], this reduction in energy corresponds to current-driven excitation of magnons with $\lambda_m \sim 8$ nm at B^*. The latter suggests that at the magnon resonance (line MM' in Fig. 2) current excites spin-wave mode with $\lambda_m = 4R/3$. The magnon resonance is expected to shift in the I-B plane along the contours of constant λ_m, which are lines parallel to $I^*(B)$ [31]. Our data are consistent with this analysis (see line MM' in Fig. 2).

Since both magnon (k_m) and phonon ($k_{\rm ph}$) wave vectors are oriented in the plane of the membrane (resonator), we might be able to satisfy conditions for the magnetoacoustic resonance when both frequencies and wavelengths of magnons and phonons are equal. In Fig. 2, these conditions correspond to the crossing points between the lines of magnon and phonon resonances $I_{m,\rm ph}(B)$, which have positive and negative slopes, respectively. Because of interactions between sound waves and spin waves, there should be a change in the dispersion laws for both sound and spin waves in the vicinity of the crossing points [38]. The latter manifests itself as deviations from the linear dependences of the corresponding $I_{m,\rm ph}(B)$.

According to this picture, the negative dips can be understood as antiresonances, i.e., when magnons and phonons suppress each other. Indeed, it is well known that the phase of a wave shifts by 180° when passing through a resonance. If there is only one (magnon or phonon) resonance, there develops a phase shift of only one of the coherent waves (magnon or phonon) but not of the other one. This situation allows formation of the antiresonance, resulting in a decrease of the contact resistance [dip in $dV/dI(I)$ in Fig. 1]. Suppression of magnons results in lines of antiresonances (dashed lines in Fig. 2 at $B > 3$ T) with positive slope. In contrast, suppressing phonons results in lines of antiresonances (dashed lines in Fig. 2 at $B > 3$ T) with negative slopes.

Finally, we address another interesting feature of our experimental data, namely, an increase in the amplitude of the magnon resonance peaks at $B > 8$ T and a slight deviation in the location of these peaks from the resonance line MM' (see Fig. 2). We have shown earlier [31] that external radiation can induce generation of phase-coherent magnons. Similarly, resonant magnon excitation may stimulate coherent magnon generation. Enhancement in the peak amplitude at high fields strongly suggests that such a swaser [2,31] condition is satisfied at high fields, i.e., the stimulated generation overcomes the dissipation. The shift of the peaks off the resonance line MM' is tentatively attributed to the different symmetries of stimulated and current-induced magnon modes.

In summary, we have shown that injection of a high current density $\sim 10^9$ A/cm^2 into a Co/Cu multilayer via a point contact can generate complex, but structured, variations of the resistance of the multilayer as both the injected current and an applied magnetic field are varied. We attribute these variations in resistance to resonant excitation of spin waves and sound waves by an electric current. We show that coupling of spin waves to sound waves in a magnetic multilayer can lead to complex structures in point-contact spectra, due to current-driven excitation of phonon and magnetoacoustic modes, which are similar to what we see. These arguments can also explain the up or down steps in resistance (peaks or dips in dV/dI) reported previously [4,7]. However, they do not directly explain the more complex fluctuation phenomena also contained in Fig. 4 of [4]. Our observations support the feasibility of various mesoscopic generators driven by an electric current, e.g., hypersound generator, spin-wave maser, etc., with potential high-frequency applications.

This work was supported in part by Russian MST under programs SAS and MESOSCOPICS, RFBR under Grant No. RFBR-01-02-16418, and by the U.S. NSF under Grants No. DMR-98-09688 and No. DMR-02-02476.

[1] J.C. Slonczewski, J. Magn. Magn. Mater. **159**, L1 (1996).
[2] L. Berger, Phys. Rev. B **54**, 9353 (1996).
[3] Y. B. Bazaliy, B. A. Jones, and S.-C. Zhang, Phys. Rev. B **57**, R3213 (1998).
[4] M. Tsoi *et al.*, Phys. Rev. Lett. **80**, 4281 (1998).
[5] J.-E. Wegrowe, D. Kelly, Y. Jaccard, Ph. Guittienne, and J.-Ph. Ansermet, Europhys. Lett. **45**, 626 (1999).
[6] J. Z. Sun, J. Magn. Magn. Mater. **202**, 157 (1999).
[7] E. B. Myers, D.C. Ralph, J. A. Katine, R. N. Louie, and R. A. Buhrman, Science **285**, 867 (1999).
[8] L. Berger, IEEE Trans. Magn. **34**, 3837 (1998).
[9] J.C. Slonczewski, J. Magn. Magn. Mater. **195**, L261 (1999).
[10] J.-E. Wegrowe, Phys. Rev. B **62**, 1067 (2000).
[11] J. Z. Sun, Phys. Rev. B **62**, 570 (2000).
[12] C. Heide, P. E. Zilberman, and R. J. Elliott, Phys. Rev. B **63**, 064424 (2001).
[13] X. Waintal, E. B. Myers, P.W. Brouwer, and D.C. Ralph, Phys. Rev. B **62**, 12317 (2000).
[14] M. Tsoi and V. Tsoi, JETP Lett. **73**, 98 (2001).
[15] L. Berger, J. Appl. Phys. **89**, 5521 (2001).
[16] Ya. B. Bazaliy, B. A. Jones, and S.C. Zhang, J. Appl. Phys. **89**, 6793 (2001).
[17] J. Miltat, G. Albuquerque, A. Thiaville, and C. Vouille, J. Appl. Phys. **89**, 6982 (2001).
[18] X. Waintal and P.W. Brouwer, Phys. Rev. B **63**, 220407 (2001).
[19] C. Heide, Phys. Rev. Lett. **87**, 197201 (2001).
[20] C. Heide, Phys. Rev. B **65**, 054401 (2002).
[21] M. D. Stiles and A. Zangwill, J. Appl. Phys. **91**, 6812 (2002).
[22] K. Xia, P. J. Kelly, G. E.W. Bauer, A. Brataas, and I. Turek, Phys. Rev. B **65**, 220401(R) (2002).
[23] S. Zhang, P. M. Levy, and A. Fert, Phys. Rev. Lett. **88**, 236601 (2002).
[24] J. C. Slonczewski, J. Magn. Magn. Mater. **247**, 324 (2002).
[25] M. D. Stiles and A. Zangwill, Phys. Rev. B **66**, 014407 (2002).
[26] K. Bussman, G. A. Prinz, S.-F. Cheng, and D. Wang, Appl. Phys. Lett. **75**, 2476 (1999).
[27] J. A. Katine, F. J. Albert, R. A. Buhrman, E. B. Myers, and D. C. Ralph, Phys. Rev. Lett. **84**, 3149 (2000).
[28] J. A. Katine, F. J. Albert, and R. A. Buhrman, Appl. Phys. Lett. **76**, 354 (2000).
[29] S. M. Rezende, F. M. de Aguiar, M. A. Lucena, and A. Azevedo, Phys. Rev. Lett. **84**, 4212 (2000).
[30] N. Garcia, I. G. Saveliev, Y.-W. Zhao, and A. Zlatkine, J. Magn. Magn. Mater. **214**, 7 (2000).
[31] M. Tsoi *et al.*, Nature (London) **406**, 46 (2000).
[32] E. B. Myers, D. C. Ralph, J. A. Katine, F. J. Albert, and R. A. Buhrman, J. Appl. Phys. **87**, 5502 (2000).
[33] F. J. Albert, J. A. Katine, R. A. Buhrman, and D. C. Ralph, Appl. Phys. Lett. **77**, 3809 (2000).
[34] J. Grollier *et al.*, Appl. Phys. Lett. **78**, 3663 (2001).
[35] J.-E. Wegrowe, D. Kelly, T. Truong, Ph. Guittienne, and J.-Ph. Ansermet, Europhys. Lett. **56**, 748 (2001).
[36] J.-E. Wegrowe, D. Kelly, X. Hoffer, Ph. Guittienne, and J.-Ph. Ansermet, J. Appl. Phys. **89**, 7127 (2001).
[37] E. B. Myers, F. J. Albert, J. C. Sankey, E. Bonet, R. A. Buhrman, and D. C. Ralph, cond-mat/0203487.
[38] A. I. Akhiezer, V. G. Bar̆yakhtar, and S.V. Peletminskii, *Spin Waves* (North-Holland, Amsterdam, 1968).
[39] Note that an excited ferromagnet affects the surrounding media. According to Newton's Third Law, one might also expect an inverse effect; that is, the media may affect the ferromagnet by exciting phonons in the magnet.
[40] S. Timoshenko, D. H. Young, and W. Weaver, Jr., *Vibration Problems in Engineering* (Wiley, New York, 1974).
[41] M. Tsoi *et al.* (to be published).